ORIGINAL ARTICLE

Fault Detection and Isolation for Wind Turbine Systems Based on Proportional Multi-Integral Observer (PMIO)

Yassine FADILI[1,*], Kaoutar LAHMADI[1], and Ismail BOUMHIDI[1]

[1] *Laboratory of Electronics, Signal-Systems and Information science (LESSI), Department of Physics, Faculty of Sciences Dhar El Mahraz , Sidi Mohammed Ben Abdellah University, B.P. 1796 , Fez-Atlas, Morocco.*

(**Received** *15th* August 2018; **Accepted** 3 January 2019; **Published on line** 1 September 2019).

*Corresponding author: fadili.m2si@gmail.com.

DOI: 10.5875/ausmt.v9i3.1917.

Abstract: This paper addresses Fault Detection and Isolation (FDI) for wind turbines based on a Proportional Multi-Integral Observer (PMIO). A wind turbine model is linearized using the Takagi-Sugeno (TS) approach based on Lyapunov stability theory and LMI condition, then the PMI observer is considered for use with the TS fuzzy model to estimate and isolate both actuator and sensor faults with the introduction of a centered noise. The kth derivatives of the actuators and sensor faults are not equal to zero but are rather bounded norms. However, based on Lyapunov stability theory and L2 performance analysis, design conditions are established through LMIs formulations. Simulation results show that our proposal outperforms some existing approaches.

Keywords: Fault Detection and Isolation (FDI); Wind Turbine System; Proportional Multi-Integral Observer (PMIO); Takagi-Sugeno (TS) approach; Lyapunov stability theory; L_2 performance analysis.

Introduction

Wind turbines represent an increasingly important source of electrical power around the world, and many wind farms are being located offshore to access stronger and more stable wind sources [5]. Such offshore installations are more difficult and costly to service than onshore turbines [7]. Efficient fault monitoring and diagnostics can potentially predict equipment failures before they occur, thus allowing for timely intervention to prevent downtime or damage [8].

To test different schemes for Fault Detection and Isolation (FDI) for an offshore wind turbine, we use a wind turbine reference model introduced in [9] using the desired detection time and false alarm rate. The benchmark model presented corresponds to a three-axis horizontal axis wind turbine with a nominal power of 4.8 MW. Some work has been achieved for FDI in wind turbine system based driven data [10]. The authors in [11] proposed a data-driven fault detection scheme with robust residual generators directly constructed from available process data. In [12] a classifier combined Bayes Statistical Algorithm, Back-propagation Neural Networks, and Decision Trees, and in [13] a Fuzzy/Bayesian network classifier was made to classify data into two classes, to determine whether the system state is defective or not. In addition to the nonlinearity of its simulation model, the high power of the noise in all the sensor signals defined in [9] generates problems in the FDI design. These factors make the FDI problem very challenging [14].The authors in [15-16] used the Kalman Filter (KF) and generalized likelihood ratio test to generation and evaluation residues. In [17], the fault diagnosis approach was combined with analytical redundancy relations (ARRs) and interval observervations. In [18], the unknown input observer was proposed to detectsensor faults in the drive train and converter subsystems of the benchmark model. Further, in [8], the Sliding Mode Observer (SMO) based estimation scheme was presented to detect, isolate and estimate sensor and actuator status in benchmark model subsystems. In addition, to solve the nonlinearity disadvantages in the simulation model [19], the authors in [20] proposed a fault diagnosis scheme based fuzzy models. This fuzzy model, in the form of a Takagi-Sugeno (T-S) prototype, represented the residual generators used for fault detection and isolation (FDI).

This paper focuses on a fault diagnosis method for the wind turbine system model developed by [19], which is linearized using the Takagi-Sugeno (T-S) approach based on Lyapunov's stability theory and LMI condition for T-S systems stability presented in [21]. Furthermore, a Proportional Multi-Integral Observer (PMIO) is considered for the T-S fuzzy model to estimate both actuator and sensor faults by introducing a centered noise. However, the k^{th} derivatives of the unknown inputs (actuators and sensor faults) are not equal to zero and are bounded norms. Based on Lyapunov's stability theory and L_2 performance analysis, the design conditions are established in LMIs formulations.

This remainder of this paper is organized as follows. In section 2, the model of the wind turbine is presented and linearized using the TS approach. In section 3, the design state feedback controller is proposed. In section 4, the structure and synthesis of PMIO are presented. Section 5 describes a simulation that compares estimation of actuator and sensor faults. Conclusion are presented in Section 6.

Wind Turbine System Modeling

Wind Turbine Basics

A wind turbine captures kinematic energy from the wind and transforms it into mechanical energy (by rotating a shaft), then into electrical energy (through a generator). As shown in Figure 1, the visible components of horizontal axis wind turbines (HAWTs) are the tower, the nacelle, and the rotor.

The wind spins the rotor on this upwind horizontal-axis turbine. The low-speed shaft transfers energy to the gearbox which drives the high speed shaft, which then drives the generator, producing electricity. In Figure 1, the yaw-actuation mechanism rotates the nacelle so that the rotor faces into the wind [22]. The modeling of the wind turbine mainly represents its

Yassine FADILI, received his M.Sc degree from Sidi Mohammed ben Abdellah University of Fez in 2014, he is currently pursuing the Ph.D. degree at Sidi Mohammed ben Abdellah University. The main research interests include nonlinear systems, Fuzzy Systems, Stability Theory, multivariable nonlinear systems ,intelligent control systems, Fault Detection and Isolation, Fault Tolerant Control.

Kaoutar LAHMADI, received his M.Sc degree from Sidi Mohammed ben Abdellah University of Fez in 2014, he is currently pursuing the Ph.D. degree at Sidi Mohammed ben Abdellah University. The main research interests include nonlinear systems, Fuzzy Systems, intelligent control systems, Fault Detection and Isolation.

Ismail BOUMHIDI, Professor of electronics at the Faculty of Sciences, Fez, Morocco. He received his Ph.D. degree from Sidi Mohamed ben Abdellah University, Faculty of sciences, in 1999. His research areas include adaptive robust control, multivariable nonlinear systems, and fuzzy logic control with applications, intelligent control systems, Fault Detection and Isolation, Fault Tolerant Control.

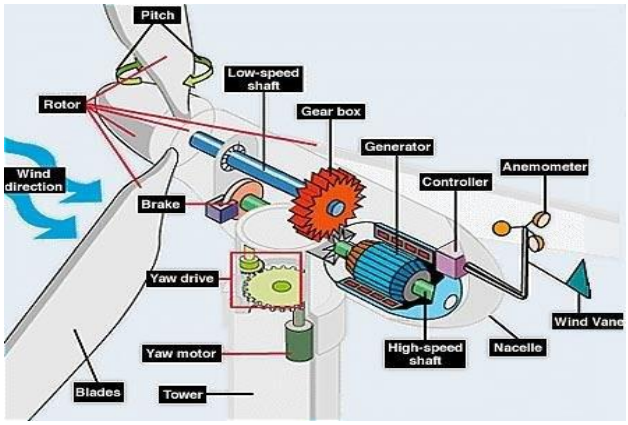

Figure 1. Wind turbine components.

aerodynamic, mechanical and electrotechnical characteristics.

Wind Turbine Modelling:

This article uses a three-bladed pitch-controlled variable speed wind turbine model with a nominal power of 4.8 MW as described in paper [23].

Aerodynamic model:

The aerodynamics of the wind turbine are modeled as a torque acting on the blades, according to:

$$\tau_r(t) = \sum_{i=1}^{3} \frac{\rho.\pi.R^3.C_q(\lambda_i(t),\beta_i(t)).\upsilon_{\omega,i}^2(t)}{6} \quad (1)$$

where $v_{\omega,i}(t)$ is the wind speed, ρ[kg/m^3] is the air density, R[m] is the rotor radius, $\beta_i(t)$ is pitch position of the blades, ω_r is the rotor speed, and $\lambda_i(t)$ is the tip speed ratio, defined as:

$$\lambda_i(t) = \frac{\omega_r(t).R}{\upsilon_{\omega,i}(t)} \quad (2)$$

Pitch system model:

For each blade, the hydraulic pitch system is modeled as a closed-loop second order transfer function between the pitch angle β_i and its reference $\beta_{i;ref}$, according to:

$$\frac{\beta_i(s)}{\beta_{i,ref}(s)} = \frac{\omega_n^2}{s^2 + 2\zeta\omega_n \cdot s + \omega_n^2} \quad (3)$$

which can be written as a differential equation:

$$\ddot{\beta}_i(t) = -2\zeta\omega_n\dot{\beta}_i(t) - \omega_n^2\beta_i(t) + \omega_n^2\beta_{i,ref}(t) \quad (4)$$

where ζ is the damping factor, and ω_n [rad/s] is the natural frequency, and i = 1, 2, 3 for three blades.

Drive train model:

The drive train by a two-mass model is modeled as follow:

$$\dot{\omega}_r(t) = \frac{1}{J_r}\tau_r(t) - \frac{K_{dt}}{J_r}\theta_\Delta(t) - (\frac{B_{dt}+B_r}{J_r})\omega_r(t) + \frac{B_{dt}}{J_r N_g}\omega_g(t) \quad (5)$$

$$\dot{\omega}_g(t) = \frac{\eta_{dt}K_{dt}}{J_g N_g}\theta_\Delta(t) - \frac{\eta_{dt}K_{dt}}{J_g N_g}\omega_r(t) + (\frac{\eta_{dt}B_{dt}}{J_g N_g^2} + \frac{B_g}{J_g})\omega_g(t) - \frac{1}{J_g}\tau_g(t) \quad (6)$$

$$\dot{\theta}_\Delta(t) = \omega_r(t) - \frac{1}{N_g}\omega_g(t) \quad (7)$$

where ωr(t) is the rotor speed, ωg(t) is the generator speed, τr(t) is the rotor torque, τg(t) is the generator torque, Jr[kg.m2] is the moment of inertia of the low-speed shaft, Kdt[Nm/rad] is the torsion stiffness of the drive train, Bdt[Nms/rad] is the torsion damping coefficient of the drive train, Br[Nms/rad] and Bg[Nms/rad] are respectively the viscous friction of the high-speed shaft of rotor and generator, Ng is the gear ratio, Jg[kg.m2] is the moment of the inertia of the high-speed shaft, ηdt is the efficiency of the drive train, and θΔ(t) is the torsion angle of the drive train.

Generator and Converter model:

The generator and converter dynamics can be modeled by the following first order transfer function:

$$\frac{\tau_g(s)}{\tau_{g,ref}(s)} = \frac{\alpha_{gc}}{s+\alpha_{gc}} \quad (8)$$

This dynamics can be approximated by a first order model with time constant t_g [19]:

$$\dot{\tau}_g(t) = -\frac{\tau_g(t)}{t_g} + \frac{\tau_{g,ref}(t)}{t_g} \quad (9)$$

The power produced by the generator is given by:

$$P_g(t) = \eta_g \cdot \omega_g(t)\,\tau_g \quad (10)$$

where α_{gc}[rad/s] is the generator and converter model parameter, η_g is the efficiency of the generator. The generator torque τ_g is controlled by the generator torque reference $\tau_{g,ref}$.

Wind turbine control:

The mean wind speed determines the area of operation of the controller and therefore of the wind turbine. As shown in Fig. 2, turbine operations fall into four distinct categories determined by wind speed: (1) cut in speed, below which wind is insufficient to drive the turbine; (2) interim area in which wind speeds are sufficient to drive the turbine but are still below nominal wind speed; (3) maximum power capture region, which begins at the minimum nominal wind speed; and (4) cutting speed, at which wind speeds are too high for safe operation. The main objective of wind turbine system operation controls is to optimize the conversion of wind energy into mechanical energy to generate electricity. These systems are characterized by nonlinear aerodynamic behaviors and depend on the uncontrollable stochastic force of the wind, using defects as a driving signal. The design of such a system, from analysis and control designs to real-world applications, requires an accurate global mathematical model of turbine dynamics. Normally, such a model is obtained by combining the models of constituent subsystems with overall wind turbines dynamics. This section describes the combination of a low speed flexible shaft model with a conceptual two-mass wind turbine model.

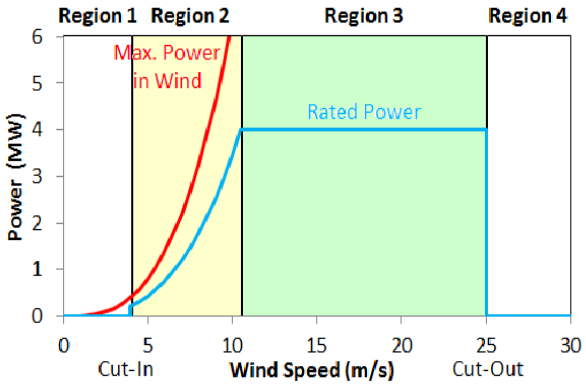

Figure 2. Wind turbine reference power curve for different wind speed zones.

Takagi-Sugeno Model of the Wind Turbine System :

State space representation of the wind turbine:

To use the Takagi-Sugeno Approach, the model is first transformed into a state space representation. We define the state and input vectors following [19]:

$$x(t) = \left[\omega_r(t)\ \ \omega_g(t)\ \ \theta_\Delta(t)\ \ \tau_g(t)\ \ \beta_1(t)\ \ \dot{\beta}_1(t)\ \ \beta_2(t)\ \ \dot{\beta}_2(t)\ \ \beta_3(t)\ \ \dot{\beta}_3(t)\right]^T \quad (11)$$

$$u(t) = \left[\tau_{g,ref}(t)\ \ \beta_{1,ref}(t)\ \ \beta_{2,ref}(t)\ \ \beta_{3,ref}(t)\right]^T \quad (12)$$

Equations (5), (6), (7), (9) and (4) provide the rankings for each blade. The model of the wind turbine can be written into a state space embedding the nonlinearities in the parameters:

$$\dot{x}(t) = A \cdot x(t) + B \cdot u(t) \quad (13)$$

$$y(t) = C \cdot x(t) \quad (14)$$

Remark 1. The nonlinear system structure presented

in (13) and (14) was studied in [19]. The nonlinearity of this structure is presented in the terms 'z_i' ((15), (16) and (17)) from the coefficient of power $C_q(\lambda_i,\beta_i)$ and the wind speed $v_{w,i}(t)$ for each blade. For this reason we used Takagi-Sugeno to solve the nonlinearity problem as shown in the following section.

Where

$$A=\begin{bmatrix} -\frac{B_{dt}+B_r}{J_r} & \frac{B_{dt}}{N_g J_r} & -\frac{K_{dt}}{J_r} & 0 & z_1(t) & 0 & z_2(t) & 0 & z_3(t) & 0 \\ -\frac{\eta_{dt}K_{dt}}{J_g N_g} & \frac{\eta_{dt}B_{dt}}{J_g N_g^2}+\frac{B_g}{J_g} & \frac{\eta_{dt}K_{dt}}{J_g N_g} & -\frac{1}{J_g} & 0 & 0 & 0 & 0 & 0 & 0 \\ 1 & -\frac{1}{N_g} & 0 & 0 & 0 & 0 & 0 & 0 & 0 & 0 \\ 0 & 0 & 0 & -\frac{1}{t_g} & 0 & 0 & 0 & 0 & 0 & 0 \\ 0 & 0 & 0 & 0 & 0 & 1 & 0 & 0 & 0 & 0 \\ 0 & 0 & 0 & 0 & -\omega_n^2 & -2\zeta\omega_n & 0 & 0 & 0 & 0 \\ 0 & 0 & 0 & 0 & 0 & 0 & 0 & 1 & 0 & 0 \\ 0 & 0 & 0 & 0 & 0 & 0 & -\omega_n^2 & -2\zeta\omega_n & 0 & 0 \\ 0 & 0 & 0 & 0 & 0 & 0 & 0 & 0 & 0 & 1 \\ 0 & 0 & 0 & 0 & 0 & 0 & 0 & 0 & -\omega_n^2 & -2\zeta\omega_n \end{bmatrix}$$

$$B=\begin{bmatrix} 0 & 0 & 0 & 0 \\ 0 & 0 & 0 & 0 \\ 0 & 0 & 0 & 0 \\ \frac{1}{t_g} & 0 & 0 & 0 \\ 0 & 0 & 0 & 0 \\ 0 & \omega_n^2 & 0 & 0 \\ 0 & 0 & 0 & 0 \\ 0 & 0 & \omega_n^2 & 0 \\ 0 & 0 & 0 & 0 \\ 0 & 0 & 0 & \omega_n^2 \end{bmatrix} \quad \text{and} \quad C=\begin{bmatrix} 1 & 0 & 0 & 0 & 0 & 0 & 0 & 0 & 0 & 0 \\ 0 & 1 & 0 & 0 & 0 & 0 & 0 & 0 & 0 & 0 \\ 0 & 0 & 0 & 1 & 0 & 0 & 0 & 0 & 0 & 0 \\ 0 & 0 & 0 & 0 & 1 & 0 & 0 & 0 & 0 & 0 \\ 0 & 0 & 0 & 0 & 0 & 0 & 1 & 0 & 0 & 0 \\ 0 & 0 & 0 & 0 & 0 & 0 & 0 & 0 & 1 & 0 \end{bmatrix}$$

And :

$$z_1(t)=\frac{\rho\cdot\pi\cdot R^3\cdot C_q(\lambda_1(t),\beta_1(t))\cdot \upsilon_{\omega,1}(t)^2}{6\cdot J_r\cdot\beta_1(t)} \quad (15)$$

$$z_2(t)=\frac{\rho\cdot\pi\cdot R^3\cdot C_q(\lambda_2(t),\beta_2(t))\cdot \upsilon_{\omega,2}(t)^2}{6\cdot J_r\cdot\beta_2(t)} \quad (16)$$

$$z_3(t)=\frac{\rho\cdot\pi\cdot R^3\cdot C_q(\lambda_3(t),\beta_3(t))\cdot \upsilon_{\omega,3}(t)^2}{6\cdot J_r\cdot\beta_3(t)} \quad (17)$$

Wind turbine fuzzy model:

The Takagi-Sugeno (T-S) model is applied using the method presented in [24]. The fuzzy model proposed by Takagi and Sugeno [25] is described by fuzzy IF-THEN rules which represent local linear input-output relations of a nonlinear system. The main feature of a Takagi-Sugeno fuzzy model is to express the local dynamics of each fuzzy implication (rule) by a linear system model. The i^{th} rules of the T-S fuzzy models are in the following form:

Model Rule i:

IF: $z_1(t)$ is $M_{i,1}$, $z_2(t)$ is $M_{i,2}$ and $z_3(t)$ is $M_{i,3}$

THEN: $\begin{cases} \dot{x}(t)=A_i\cdot x(t)+B\cdot u(t) \\ y(t)=C\cdot x(t) \end{cases}$ (18)

Where i = 1, 2, ..., r .

Here, $M_{i,j}$ is the fuzzy set and r = 2^3 is the number of model rules, $A_i \in R^{n\times n}$, $z_1(t)$, $z_2(t)$, $z_3(t)$ are known premise variables that can be functions of the state variables, external disturbances, and/or time. Given a pair of x(t); u(t), the final outputs of the fuzzy systems are inferred as follows:

$$\dot{x}(t)=\frac{\sum_{i=1}^{r}\omega_i(z(t))(A_i\cdot x(t)+B\cdot u(t))}{\sum_{i=1}^{r}\omega_i(z(t))} \quad (19)$$

which can be rewritten as :

$$\dot{x}(t)=\sum_{i=1}^{r}h_i(z(t))(A_i\cdot x(t)+B\cdot u(t)) \quad (20)$$

Where : $z(t)=\begin{bmatrix} z_1(t) & z_2(t) & z_3(t) \end{bmatrix}$ (21)

$$\omega_i(z(t))=\prod_{j=1}^{3}M_{i,j}(z_j(t)) \quad (22)$$

$$h_i(t)=\frac{\omega_i(z(t))}{\sum_{i=1}^{r}\omega_i(z(t))} \quad (23)$$

For all t, the term $M_{i,j}(z_j(t))$ is the grade of membership of $z_j(t)$ in $M_{i,j}$. Since:

$$\sum_{i=1}^{r}\omega_i(z(t))>0 \quad (24)$$

where $\sum_{i=1}^{r}\omega_i(z(t))\geq 0$; i=1, 2, ..., 8.

and $\sum_{i=1}^{r}h_i(z(t))>0$ (25)

where $\sum_{i=1}^{r}h_i(z(t))\geq 0$; i=1, 2, ..., 8.

From Eqs. (20) to (23), $z_1(t) \in [z_{1,min};z_{1,max}]$, $z_2(t) \in [z_{2,min}; z_{2,max}]$, $z_3(t) \in [z_{3,min}; z_{3,max}]$ is bounded. From the maximum and minimum values $z_1(t)$, $z_2(t)$ and $z_3(t)$ can be represented by:

$$z_1(t)=\frac{\rho\pi R^3 C_q(\lambda_1(t),\beta_1(t))\upsilon_{\omega,1}(t)^2}{6J_r\beta_1(t)}=M_1(z_1(t))\cdot z_{1,\max}+M_2(z_1(t))\cdot z_{1,\min} \quad (26)$$

$$z_2(t)=\frac{\rho\pi R^3 C_q(\lambda_2(t),\beta_2(t))\upsilon_{\omega,2}(t)^2}{6J_r\beta_2(t)}=N_1(z_2(t))\cdot z_{2,\max}+N_2(z_2(t))\cdot z_{2,\min} \quad (27)$$

$$z_3(t)=\frac{\rho\pi R^3 C_q(\lambda_3(t),\beta_3(t))\upsilon_{\omega,3}(t)^2}{6J_r\beta_3(t)}=L_1(z_3(t))\cdot z_{3,\max}+L_2(z_3(t))\cdot z_{3,\min} \quad (28)$$

Therefore the membership functions can be calculated as:

$$\begin{cases} M_1=\dfrac{z_1-z_{1,\min}}{z_{1,\max}-z_{1,\min}} \\ M_2=\dfrac{z_{1,\max}-z_1}{z_{1,\max}-z_{1,\min}} \end{cases} \quad (29)$$

$$\begin{cases} N_1=\dfrac{z_2-z_{2,\min}}{z_{2,\max}-z_{2,\min}} \\ N_2=\dfrac{z_{2,\max}-z_2}{z_{2,\max}-z_{2,\min}} \end{cases} \quad (30)$$

$$\begin{cases} L_1=\dfrac{z_3-z_{3,\min}}{z_{3,\max}-z_{3,\min}} \\ L_2=\dfrac{z_{3,\max}-z_3}{z_{3,\max}-z_{3,\min}} \end{cases} \quad (31)$$

The membership functions are specified as shown in Table 1 based $z_{i,max}$ and $z_{i,min}$:

Table 1. Fuzzy Model.

Sets	$z_1(t)$	$z_2(t)$	$z_3(t)$	*A matrix*
Rule 1	$z_{1,min}(t)$	$z_{2,min}(t)$	$z_{3,min}(t)$	A_1
Rule 2	$z_{1,max}(t)$	$z_{2,min}(t)$	$z_{3,min}(t)$	A_2
Rule 3	$z_{1,min}(t)$	$z_{2,max}(t)$	$z_{3,min}(t)$	A_3
Rule 4	$z_{1,max}(t)$	$z_{2,max}(t)$	$z_{3,min}(t)$	A_4
Rule 5	$z_{1,min}(t)$	$z_{2,min}(t)$	$z_{3,max}(t)$	A_5
Rule 6	$z_{1,max}(t)$	$z_{2,min}(t)$	$z_{3,max}(t)$	A_6
Rule 7	$z_{1,min}(t)$	$z_{2,max}(t)$	$z_{3,max}(t)$	A_7
Rule 8	$z_{1,max}(t)$	$z_{2,max}(t)$	$z_{3,max}(t)$	A_8

Then, the matrices of the local models are:

$$A_1=\begin{bmatrix} -\frac{B_{dt}+B_r}{J_r} & \frac{B_{dt}}{N_gJ_r} & -\frac{K_{dt}}{J_r} & 0 & z_{1,\min} & 0 & z_{2,\min} & 0 & z_{3,\min} & 0 \\ -\frac{\eta_{dt}K_{dt}}{J_gN_g} & \frac{\eta_{dt}B_{dt}}{J_gN_g^2}+\frac{B_g}{J_g} & \frac{\eta_{dt}K_{dt}}{J_gN_g} & -\frac{1}{J_g} & 0 & 0 & 0 & 0 & 0 & 0 \\ 1 & -\frac{1}{N_g} & 0 & 0 & 0 & 0 & 0 & 0 & 0 & 0 \\ 0 & 0 & 0 & -\frac{1}{t_g} & 0 & 0 & 0 & 0 & 0 & 0 \\ 0 & 0 & 0 & 0 & 0 & 1 & 0 & 0 & 0 & 0 \\ 0 & 0 & 0 & 0 & -\omega_n^2 & -2\zeta\omega_n & 0 & 0 & 0 & 0 \\ 0 & 0 & 0 & 0 & 0 & 0 & 0 & 1 & 0 & 0 \\ 0 & 0 & 0 & 0 & 0 & 0 & -\omega_n^2 & -2\zeta\omega_n & 0 & 0 \\ 0 & 0 & 0 & 0 & 0 & 0 & 0 & 0 & 0 & 1 \\ 0 & 0 & 0 & 0 & 0 & 0 & 0 & 0 & -\omega_n^2 & -2\zeta\omega_n \end{bmatrix}$$

$$A_2=\begin{bmatrix} -\frac{B_{dt}+B_r}{J_r} & \frac{B_{dt}}{N_gJ_r} & -\frac{K_{dt}}{J_r} & 0 & z_{1,\max} & 0 & z_{2,\min} & 0 & z_{3,\min} & 0 \\ -\frac{\eta_{dt}K_{dt}}{J_gN_g} & \frac{\eta_{dt}B_{dt}}{J_gN_g^2}+\frac{B_g}{J_g} & \frac{\eta_{dt}K_{dt}}{J_gN_g} & -\frac{1}{J_g} & 0 & 0 & 0 & 0 & 0 & 0 \\ 1 & -\frac{1}{N_g} & 0 & 0 & 0 & 0 & 0 & 0 & 0 & 0 \\ 0 & 0 & 0 & -\frac{1}{t_g} & 0 & 0 & 0 & 0 & 0 & 0 \\ 0 & 0 & 0 & 0 & 0 & 1 & 0 & 0 & 0 & 0 \\ 0 & 0 & 0 & 0 & -\omega_n^2 & -2\zeta\omega_n & 0 & 0 & 0 & 0 \\ 0 & 0 & 0 & 0 & 0 & 0 & 0 & 1 & 0 & 0 \\ 0 & 0 & 0 & 0 & 0 & 0 & -\omega_n^2 & -2\zeta\omega_n & 0 & 0 \\ 0 & 0 & 0 & 0 & 0 & 0 & 0 & 0 & 0 & 1 \\ 0 & 0 & 0 & 0 & 0 & 0 & 0 & 0 & -\omega_n^2 & -2\zeta\omega_n \end{bmatrix}$$

$$A_3=\begin{bmatrix} -\frac{B_{dt}+B_r}{J_r} & \frac{B_{dt}}{N_gJ_r} & -\frac{K_{dt}}{J_r} & 0 & z_{1,\min} & 0 & z_{2,\max} & 0 & z_{3,\min} & 0 \\ -\frac{\eta_{dt}K_{dt}}{J_gN_g} & \frac{\eta_{dt}B_{dt}}{J_gN_g^2}+\frac{B_g}{J_g} & \frac{\eta_{dt}K_{dt}}{J_gN_g} & -\frac{1}{J_g} & 0 & 0 & 0 & 0 & 0 & 0 \\ 1 & -\frac{1}{N_g} & 0 & 0 & 0 & 0 & 0 & 0 & 0 & 0 \\ 0 & 0 & 0 & -\frac{1}{t_g} & 0 & 0 & 0 & 0 & 0 & 0 \\ 0 & 0 & 0 & 0 & 0 & 1 & 0 & 0 & 0 & 0 \\ 0 & 0 & 0 & 0 & -\omega_n^2 & -2\zeta\omega_n & 0 & 0 & 0 & 0 \\ 0 & 0 & 0 & 0 & 0 & 0 & 0 & 1 & 0 & 0 \\ 0 & 0 & 0 & 0 & 0 & 0 & -\omega_n^2 & -2\zeta\omega_n & 0 & 0 \\ 0 & 0 & 0 & 0 & 0 & 0 & 0 & 0 & 0 & 1 \\ 0 & 0 & 0 & 0 & 0 & 0 & 0 & 0 & -\omega_n^2 & -2\zeta\omega_n \end{bmatrix}$$

$$A_4=\begin{bmatrix}
-\frac{B_{dt}+B_r}{J_r} & \frac{B_{dt}}{N_gJ_r} & -\frac{K_{dt}}{J_r} & 0 & z_{1,\max} & 0 & z_{2,\max} & 0 & z_{3,\min} & 0\\
-\frac{\eta_{dt}K_{dt}}{J_gN_g} & \frac{\eta_{dt}B_{dt}}{J_gN_g^2}+\frac{B_g}{J_g} & \frac{\eta_{dt}K_{dt}}{J_gN_g} & -\frac{1}{J_g} & 0 & 0 & 0 & 0 & 0 & 0\\
1 & -\frac{1}{N_g} & 0 & 0 & 0 & 0 & 0 & 0 & 0 & 0\\
0 & 0 & 0 & -\frac{1}{t_g} & 0 & 0 & 0 & 0 & 0 & 0\\
0 & 0 & 0 & 0 & 0 & 1 & 0 & 0 & 0 & 0\\
0 & 0 & 0 & 0 & -\omega_n^2 & -2\zeta\omega_n & 0 & 0 & 0 & 0\\
0 & 0 & 0 & 0 & 0 & 0 & 0 & 1 & 0 & 0\\
0 & 0 & 0 & 0 & 0 & 0 & -\omega_n^2 & -2\zeta\omega_n & 0 & 0\\
0 & 0 & 0 & 0 & 0 & 0 & 0 & 0 & 0 & 1\\
0 & 0 & 0 & 0 & 0 & 0 & 0 & 0 & -\omega_n^2 & -2\zeta\omega_n
\end{bmatrix}$$

$$A_5=\begin{bmatrix}
-\frac{B_{dt}+B_r}{J_r} & \frac{B_{dt}}{N_gJ_r} & -\frac{K_{dt}}{J_r} & 0 & z_{1,\min} & 0 & z_{2,\min} & 0 & z_{3,\max} & 0\\
-\frac{\eta_{dt}K_{dt}}{J_gN_g} & \frac{\eta_{dt}B_{dt}}{J_gN_g^2}+\frac{B_g}{J_g} & \frac{\eta_{dt}K_{dt}}{J_gN_g} & -\frac{1}{J_g} & 0 & 0 & 0 & 0 & 0 & 0\\
1 & -\frac{1}{N_g} & 0 & 0 & 0 & 0 & 0 & 0 & 0 & 0\\
0 & 0 & 0 & -\frac{1}{t_g} & 0 & 0 & 0 & 0 & 0 & 0\\
0 & 0 & 0 & 0 & 0 & 1 & 0 & 0 & 0 & 0\\
0 & 0 & 0 & 0 & -\omega_n^2 & -2\zeta\omega_n & 0 & 0 & 0 & 0\\
0 & 0 & 0 & 0 & 0 & 0 & 0 & 1 & 0 & 0\\
0 & 0 & 0 & 0 & 0 & 0 & -\omega_n^2 & -2\zeta\omega_n & 0 & 0\\
0 & 0 & 0 & 0 & 0 & 0 & 0 & 0 & 0 & 1\\
0 & 0 & 0 & 0 & 0 & 0 & 0 & 0 & -\omega_n^2 & -2\zeta\omega_n
\end{bmatrix}$$

$$A_6=\begin{bmatrix}
-\frac{B_{dt}+B_r}{J_r} & \frac{B_{dt}}{N_gJ_r} & -\frac{K_{dt}}{J_r} & 0 & z_{1,\max} & 0 & z_{2,\min} & 0 & z_{3,\max} & 0\\
-\frac{\eta_{dt}K_{dt}}{J_gN_g} & \frac{\eta_{dt}B_{dt}}{J_gN_g^2}+\frac{B_g}{J_g} & \frac{\eta_{dt}K_{dt}}{J_gN_g} & -\frac{1}{J_g} & 0 & 0 & 0 & 0 & 0 & 0\\
1 & -\frac{1}{N_g} & 0 & 0 & 0 & 0 & 0 & 0 & 0 & 0\\
0 & 0 & 0 & -\frac{1}{t_g} & 0 & 0 & 0 & 0 & 0 & 0\\
0 & 0 & 0 & 0 & 0 & 1 & 0 & 0 & 0 & 0\\
0 & 0 & 0 & 0 & -\omega_n^2 & -2\zeta\omega_n & 0 & 0 & 0 & 0\\
0 & 0 & 0 & 0 & 0 & 0 & 0 & 1 & 0 & 0\\
0 & 0 & 0 & 0 & 0 & 0 & -\omega_n^2 & -2\zeta\omega_n & 0 & 0\\
0 & 0 & 0 & 0 & 0 & 0 & 0 & 0 & 0 & 1\\
0 & 0 & 0 & 0 & 0 & 0 & 0 & 0 & -\omega_n^2 & -2\zeta\omega_n
\end{bmatrix}$$

$$A_7=\begin{bmatrix}
-\frac{B_{dt}+B_r}{J_r} & \frac{B_{dt}}{N_gJ_r} & -\frac{K_{dt}}{J_r} & 0 & z_{1,\min} & 0 & z_{2,\max} & 0 & z_{3,\max} & 0\\
-\frac{\eta_{dt}K_{dt}}{J_gN_g} & \frac{\eta_{dt}B_{dt}}{J_gN_g^2}+\frac{B_g}{J_g} & \frac{\eta_{dt}K_{dt}}{J_gN_g} & -\frac{1}{J_g} & 0 & 0 & 0 & 0 & 0 & 0\\
1 & -\frac{1}{N_g} & 0 & 0 & 0 & 0 & 0 & 0 & 0 & 0\\
0 & 0 & 0 & -\frac{1}{t_g} & 0 & 0 & 0 & 0 & 0 & 0\\
0 & 0 & 0 & 0 & 0 & 1 & 0 & 0 & 0 & 0\\
0 & 0 & 0 & 0 & -\omega_n^2 & -2\zeta\omega_n & 0 & 0 & 0 & 0\\
0 & 0 & 0 & 0 & 0 & 0 & 0 & 1 & 0 & 0\\
0 & 0 & 0 & 0 & 0 & 0 & -\omega_n^2 & -2\zeta\omega_n & 0 & 0\\
0 & 0 & 0 & 0 & 0 & 0 & 0 & 0 & 0 & 1\\
0 & 0 & 0 & 0 & 0 & 0 & 0 & 0 & -\omega_n^2 & -2\zeta\omega_n
\end{bmatrix}$$

$$A_8=\begin{bmatrix}
-\frac{B_{dt}+B_r}{J_r} & \frac{B_{dt}}{N_gJ_r} & -\frac{K_{dt}}{J_r} & 0 & z_{1,\max} & 0 & z_{2,\max} & 0 & z_{3,\max} & 0\\
-\frac{\eta_{dt}K_{dt}}{J_gN_g} & \frac{\eta_{dt}B_{dt}}{J_gN_g^2}+\frac{B_g}{J_g} & \frac{\eta_{dt}K_{dt}}{J_gN_g} & -\frac{1}{J_g} & 0 & 0 & 0 & 0 & 0 & 0\\
1 & -\frac{1}{N_g} & 0 & 0 & 0 & 0 & 0 & 0 & 0 & 0\\
0 & 0 & 0 & -\frac{1}{t_g} & 0 & 0 & 0 & 0 & 0 & 0\\
0 & 0 & 0 & 0 & 0 & 1 & 0 & 0 & 0 & 0\\
0 & 0 & 0 & 0 & -\omega_n^2 & -2\zeta\omega_n & 0 & 0 & 0 & 0\\
0 & 0 & 0 & 0 & 0 & 0 & 0 & 1 & 0 & 0\\
0 & 0 & 0 & 0 & 0 & 0 & -\omega_n^2 & -2\zeta\omega_n & 0 & 0\\
0 & 0 & 0 & 0 & 0 & 0 & 0 & 0 & 0 & 1\\
0 & 0 & 0 & 0 & 0 & 0 & 0 & 0 & -\omega_n^2 & -2\zeta\omega_n
\end{bmatrix}$$

Fuzzy Controller Design:

A state feedback controller is designed based on the wind turbine TS model cited in the previous section using a design procedure called "parallel distributed compensation" (PDC) [27]. This model-based design procedure was proposed in [26].

In the PDC design, each control rule is designed from the corresponding rule of a T-S fuzzy model. For the fuzzy model (18), the following fuzzy controller is built via the PDC:

Control Rule i:

IF: $z_1(t)$ is $M_{i,1}$, $z_2(t)$ is $M_{i,2}$ and $z_3(t)$ is $M_{i,3}$

THEN: $u(t)=-T_i\cdot x(t)$; i=1, 2, ..., 8

where T_i is the feedback control gain, and can be described a fuzzy control rule. The overall fuzzy controller is represented by:

$$u(t) = -\frac{\sum_{i=1}^{r} \omega_i(z(t)) \cdot T_i \cdot x(t)}{\sum_{i=1}^{r} \omega_i(z(t))} = -\sum_{i=1}^{r} h_i(z(t)) \cdot T_i \cdot x(t) \quad (32)$$

Theorem 1. The design is based on the Lyapunov stability theory and LMI condition for stability of T-S systems in [21]. The LMI region stabilization problem in the case of S(α,r,θ) has a solution if and only if there exists a symmetric positive definite matrix X_i and a matrix Y_i satisfying:

$$A_i X_i + B Y_i + X_i A_i^T + Y_i^T B^T + 2\alpha X_i \prec 0 \quad (33)$$

$$\begin{bmatrix} -rX_i & qX_i + A_i X_i - BY_i \\ qX_i + X_i A_i^T + Y_i^T B^T & -rX_i \end{bmatrix} \prec 0 \quad (34)$$

$$\begin{bmatrix} (A_i X_i + BY_i + X_i A_i^T + Y_i^T B^T)\sin(\theta) & (A_i X_i + BY_i - (X_i A_i^T + Y_i^T B^T))\cos(\theta) \\ (A_i X_i + BY_i - (X_i A_i^T + Y_i^T B^T))\cos(\theta) & (A_i X_i + BY_i + X_i A_i^T + Y_i^T B^T)\sin(\theta) \end{bmatrix} \prec 0 \quad (35)$$

The solution to our problem is given by :

$$T_i = Y_i X_i^{-1} \quad (36)$$

where α is the minimum response speed, r is the maximum response speed, and θ is the overshoot. The LMI region S is shown in the following Figure 3:

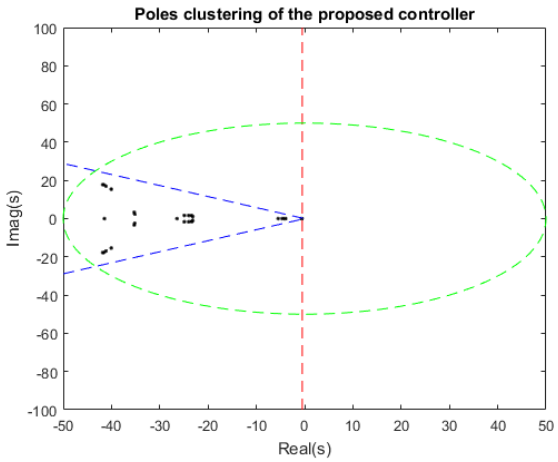

Figure 3. Poles in the LMI region S(α, r, θ).

Remark 2. All the poles are indeed located in the LMI region S(α,r,θ) as show in Figure 3, which assures system stability (20).

PMI Observer Design:

From Eqs. (14) and (20), the wind turbine T-S fuzzy model can be rewritten with the noise and the unmeasurable premise variables subject to faults and effect both actuator and sensor as follows:

$$\begin{cases} \dot{x}(t) = \sum_{i=1}^{8} h_i(z(t))(A_i \cdot x(t) + B \cdot u(t) + F_i \cdot f_a(t) + R \cdot \omega(t)) \\ y(t) = C \cdot x(t) + F \cdot f_s(t) + H \cdot \omega(t) \end{cases} \quad (37)$$

where x(t) ∈ R^n represents the state vector, u(t) ∈ R^{nu} is the input vector, $f_a(t) \in R^{nfa}$ and $f_s(t) \in R^{nfs}$ are respectively the actuators and sensors faults vectors, w(t) ∈ R^{nw} is measurement noise vector, and y(t) ∈ R^{ny} and represents the output vector. $A_i \in R^{n \times n}$ are the state matrices, B ∈ $R^{n \times nu}$ is the input matrices, C ∈ $R^{ny \times n}$ is the output matrix, $F_i \in R^{n \times nfa}$ and F ∈ $R^{ny \times nfs}$ are the faults matrices, and R ∈ $R^{n \times nw}$ and H ∈ $R^{ny \times nw}$ are the disturbance matrix.

The $h_i(z(t))$ represents the membership functions which depend on the unmeasurable premise, state x(t) of the system. These functions satisfy the convex sum property:

$$\begin{cases} \sum_{i=1}^{8} h_i(z(t)) = 1, & \forall t \geq 0 \\ 0 \leq h_i(z(t)) \leq 1, & \text{for i=1, 2, ..., 8} \end{cases} \quad (38)$$

Hypothesis 1. The faults are assumed to be time-varying signals whose k^{th} time derivatives are bounded by f_0. The following notations are used:

$$\begin{cases} \dot{f}(t) = f_1(t) \\ \dot{f}_1(t) = f_1(t) \\ \quad \vdots \\ \dot{f}_{k-1}(t) = f_k(t) \\ f_k(t) \leq 0 \end{cases} \quad (39)$$

Remark 3. This assumption allows for the consideration of a wide range of actuator and sensor faults [28].

To simultaneously estimate the actuator and sensor faults, the system (37) is transformed to an augmented state using a new state f(t) thatassumes the fault actuator and sensor of the system is defined by:

$f(t) = \begin{bmatrix} f_a(t) \\ f_s(t) \end{bmatrix}$; Where f(t) ∈ R^{nf}.

The augmented system in the fault term can be represented as follows:

$$\begin{cases} \dot{x}(t) = \sum_{i=1}^{8} h_i(z(t))(A_i \cdot x(t) + B \cdot u(t) + \bar{F}_i \cdot f(t) + R \cdot \omega(t)) \\ y(t) = C \cdot x(t) + \bar{F} \cdot f(t) + H \cdot \omega(t) \end{cases} \quad (40)$$

with $n_f = n_{fa} + n_{fs}$ and $\bar{F}_i = \begin{bmatrix} F_i \\ 0 \end{bmatrix}; \bar{F} = \begin{bmatrix} 0 \\ F \end{bmatrix}$.

The system given by (40) can then be augmented as follows:

$$\begin{cases} \dot{x}_a(t) = \sum_{i=1}^{8} h_i(z(t))(\tilde{A}_i \cdot x_a(t) + \tilde{B} \cdot u_a(t) + \tilde{R} \cdot \omega_a(t)) \\ y(t) = \tilde{C} \cdot x_a(t) + \tilde{H} \cdot \omega_a(t) \end{cases} \quad (41)$$

where $\tilde{A}_i = \begin{bmatrix} A_i & \bar{F}_i & 0 & \cdots & 0 & 0 \\ 0 & 0 & I_{n_f} & \cdots & 0 & 0 \\ 0 & 0 & 0 & \ddots & 0 & 0 \\ \vdots & \vdots & \vdots & \vdots & \vdots & \vdots \\ 0 & 0 & 0 & 0 & 0 & I_{n_f} \\ 0 & 0 & 0 & 0 & 0 & 0 \end{bmatrix}$, $x_a(t) = \begin{pmatrix} x(t) \\ f(t) \\ f_1(t) \\ \vdots \\ f_{k-1}(t) \end{pmatrix}$

$\tilde{B} = \begin{bmatrix} B \\ 0 \\ \vdots \\ 0 \end{bmatrix}$, $u_a(t) = \begin{pmatrix} u(t) \\ 0 \\ \vdots \\ 0 \end{pmatrix}$, $\tilde{R} = \begin{bmatrix} R \\ 0 \\ \vdots \\ 0 \end{bmatrix}$, $\omega_a(t) = \begin{pmatrix} \omega(t) \\ 0 \\ \vdots \\ 0 \end{pmatrix}$

and $\tilde{C} = \begin{bmatrix} C & \bar{F} & 0 & \cdots & 0 \end{bmatrix}$.

The considered PMI observer simultaneously provides the states and actuator and sensor faults in the presence of unmeasurable premise variables presented in system (40) [29], and are described as follows:

$$\begin{cases} \dot{\hat{x}}(t) = \sum_{i=1}^{8} h_i(z(t))(A_i \cdot x(t) + B \cdot u(t) + \bar{F}_i \cdot \hat{f}(t) + L_{p_i} \cdot (y(t) - \hat{y}(t))) \\ \hat{y}(t) = C \cdot x(t) + \bar{F} \cdot \hat{f}(t) \end{cases} \quad (42)$$

where $\hat{f}(t)$ is obtained by the PMI observer as follows:

$$\begin{cases} \dot{\hat{f}}_j(t) = \sum_{i=1}^{8} h_i(z(t))(f_{j+1}(t) + L_{I_i} \cdot (y(t) - \hat{y}(t))) \;\; ; \; j = 1, \ldots, k-1 \\ \dot{\hat{f}}(t) = \sum_{i=1}^{8} h_i(z(t))(f_1(t) + L_{I_i} \cdot (y(t) - \hat{y}(t))) \end{cases} \quad (43)$$

To the augmented system presented in (41), the observer (42) becomes:

$$\begin{cases} \dot{\hat{x}}_a(t) = \sum_{i=1}^{8} h_i(z(t))(\tilde{A}_i \cdot x_a(t) + \tilde{B} \cdot u_a(t) + \tilde{L}_i \cdot (y(t) - \hat{y}(t))) \\ \hat{y}(t) = \tilde{C} \cdot x_a(t) \end{cases} \quad (44)$$

where $\tilde{L}_i = \begin{bmatrix} L_{p_i}^T & L_{I_i}^T & L_{I_i}^{1\,T} & \cdots & L_{I_i}^{k-2\,T} & L_{I_i}^{k-1\,T} \end{bmatrix}^T$.

The estimation error of the state and unknown inputs and their derivatives is denoted as $e_a(t) = x_a(t) - \hat{x}_a(t)$. Using the system (41) and the observer (44), the estimation error dynamics obeys the following differential equation:

$$\dot{e}_a(t) = \sum_{i=1}^{8} h_i(z(t))((\tilde{A}_i - \tilde{L}_i\tilde{C}) \cdot e_a(t) + (\tilde{R} - \tilde{L}_i\tilde{H}) \cdot \omega_a(t)) \quad (45)$$

The aim is to synthesize the gains $\tilde{L}_i$ of the observer to ensure the stability of the system (45) generating the estimation error and to guarantee an attenuation rate γ of the disturbances transfer $\omega_a(t)$ to error $e_a(t)$. This result is translated by the following constraints:

$$\lim_{t \to +\infty} e_a(t) = 0 \;\; ; \;\; \omega_a(t) = 0 \;\; ; \;\; t \geq 0 \quad (46)$$

$$\frac{\|e_a(t)\|_2}{\|\omega_a(t)\|_2} = \gamma \;\; ; \;\; \omega_a(t) \neq 0 \;\; ; \;\; t \geq 0 \quad (47)$$

Theorem 2. The system (45) is asymptotically stable and the L_2 performance is guaranteed with an attenuation level $\gamma > 0$, if there exists a matrix $P = P^T > 0$, with $P \in R^{(n+knf)\times(n+knf)}$, and the matrix $\tilde{K}_i \in R^{(n+knf)\times nf}$ such that for all i = 1, ..., 8 the following minimization problem holds:

$$\min(\gamma)$$
$$\begin{bmatrix} \tilde{A}_i^T P + P\tilde{A}_i - \tilde{K}_i\tilde{C} - \tilde{C}\tilde{K}_i^T + I & P\tilde{R}_i - \tilde{K}_i\tilde{H} \\ \tilde{R}_i^T P - \tilde{H}^T\tilde{K}_i^T & -\gamma^2 I \end{bmatrix} \prec 0 \quad (48)$$

Then, the gains of the PMI observer are computed by:

$$\tilde{L}_i = P^{-1}\tilde{K}_i \quad (49)$$

Proof 1. Consider the quadratic Lyapunov's function follows:

$$V(e_a(t)) = e_a^T(t)(P)e_a(t) \quad (50)$$

The time-derivative of the quadratic Lyapunov function (45) leads to:

$$\dot{V}(e_a(t)) = \dot{e}_a^T(t) \cdot P \cdot e_a(t) + e_a^T(t) \cdot P \cdot \dot{e}_a(t) \quad (51)$$

By substituting $\dot{e}_a(t)$ (45) in (51), the time-derivative of the quadratic Lyapunov function becomes:

$$\dot{V}(e_a(t)) = \sum_{i=1}^{8} h_i(z(t))(e_a^T(t)(\tilde{A}_i^T P + P\tilde{A}_i - \tilde{K}_i\tilde{C} - \tilde{C}^T\tilde{K}_i^T)e_a(t) \\ \omega_a^T(t)(\tilde{R}_i^T P - \tilde{H}^T\tilde{K}_i^T)e_a(t) + e_a(t)(P\tilde{R}_i - \tilde{K}_i\tilde{H})\omega_a(t)) \quad (52)$$

The objective is to attenuate the effect of the disturbance $\omega_a(t)$ on $e_a(t)$:

$$\frac{\|e_a\|_2}{\|\omega_a\|_2} \prec \gamma \;;\; \|\omega_a\|_2 \neq 0 \;;\; \gamma \succ 0 \quad (53)$$

while ensuring the stability of the augmented system (45). As already mentioned, the following condition must be met:

$$\dot{V}(e_a(t)) + e_a^T(t)e_a(t) - \gamma\omega_a^T(t)\omega_a(t) \prec 0 \quad (54)$$

By substituting (52), we obtain:

$$\sum_{i=1}^{8} h_i(z(t))(e_a^T(t)(\tilde{A}_i^T P + P\tilde{A}_i - \tilde{K}_i\tilde{C} - \tilde{C}^T\tilde{K}_i^T)e_a(t) + e_a^T(t)e_a(t) \\ \omega_a^T(t)(\tilde{R}_i^T P - \tilde{H}^T\tilde{K}_i^T)e_a(t) + e_a(t)(P\tilde{R}_i - \tilde{K}_i\tilde{H})\omega_a(t)) - \gamma^2\omega_a^T(t)\omega_a(t) \prec 0 \quad (55)$$

which can be put in the form:

$$\sum_{i=1}^{8} h_i(z(t))\tilde{r}^T(t)\Xi_i\tilde{r}(t) \prec 0 \quad (56)$$

where $\Xi_i = \begin{bmatrix} \tilde{A}_i^T P + P\tilde{A}_i - \tilde{K}_i\tilde{C} - \tilde{C}\tilde{K}_i^T + I & P\tilde{R}_i - \tilde{K}_i\tilde{H} \\ \tilde{R}_i^T P - \tilde{H}^T\tilde{K}_i^T & -\gamma^2 I \end{bmatrix}$

and $\tilde{r}(t) = \begin{pmatrix} e_a(t) \\ \omega_a(t) \end{pmatrix}$

The sufficient condition for (48) to be verified is:

$$\begin{bmatrix} \tilde{A}_i^T P + P\tilde{A}_i - \tilde{K}_i\tilde{C} - \tilde{C}\tilde{K}_i^T + I & P\tilde{R}_i - \tilde{K}_i\tilde{H} \\ \tilde{R}_i^T P - \tilde{H}^T\tilde{K}_i^T & -\gamma^2 I \end{bmatrix} \prec 0 \;,\; \forall i \in \{1,\ldots,8\} \quad (57)$$

Simulations Results:

The proposed wind turbine controller is implemented with a sampling frequency of 100 Hz. The controller starts in mode 1. Figure 4 shows the evolution over time of the wind speed sequence $v_\omega(t)$ in the proposed model (the input). Figure 5 shows the evolution over time of the proposed centered noise $\omega(t)$. All simulations are taken for 4400s. The simulation results show that our proposed controller outperforms some existing approaches. The following subsection presents simulation results for the estimation of states, actuator and sensor faults as follows:

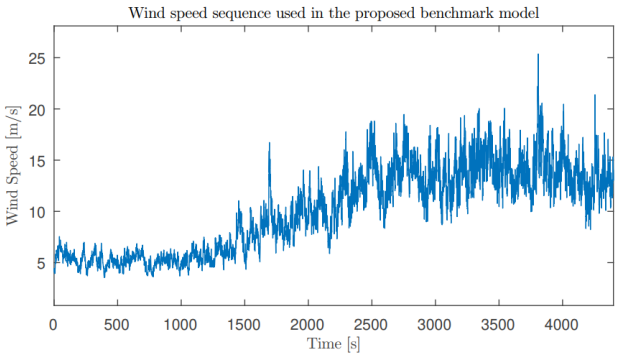

Figure 4. Wind speed sequence $\upsilon_\omega(t)$ used in the proposed wind turbine system benchmark model.

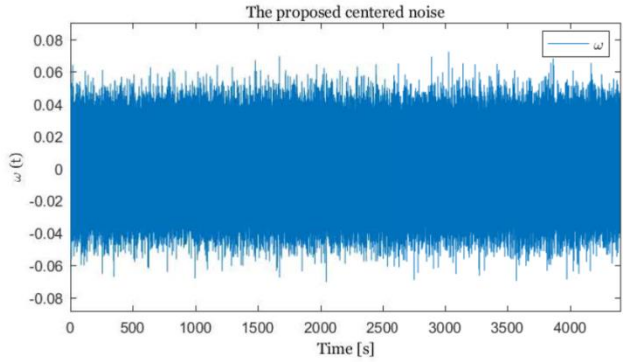

Figure 5. Proposed centered noise $\omega(t)$ in terms of time to the proposed wind turbine system benchmark model.

State estimation:

The wind turbine system used in this run is composed of a three pitch actuator system, the generator system and the Drive Train system. Solving the LMIs constraints (48) of theorem 2 thus leads to PMI observer gain.

where $F_i = \begin{bmatrix} 0.06 \\ 6 \\ \frac{1}{6} \\ 89 \\ 0.01 \\ 0.001 \\ 0.01 \\ 0.001 \\ 0.01 \\ 0.001 \end{bmatrix}$, $F = \begin{bmatrix} -0.06 \\ -6 \\ -89 \\ -0.01 \\ -0.01 \\ -0.01 \end{bmatrix}$ and $H = \begin{bmatrix} 0.5 \\ 8 \\ 0.5 \\ 0.25 \\ 0.25 \\ 0.25 \end{bmatrix}$

Using the proposed PMIO above, each state will be estimated by itself, the actuator and sensor faults as follows:

Pitch actuators system 1 angle β1

Figure 6 and 7 respectively show the pitch actuators system 1 angle estimation $\hat{\beta}_1$ and the error estimation $e_{\hat{\beta}_1}$ with the proposed PMI observer, where $\hat{\beta}_1 = \beta_{1_{est}}$ and $e_{\beta_1} = \beta_1 - \hat{\beta}_1$. The simulation results show that our proposed approach outperforms some existing approaches [8]:

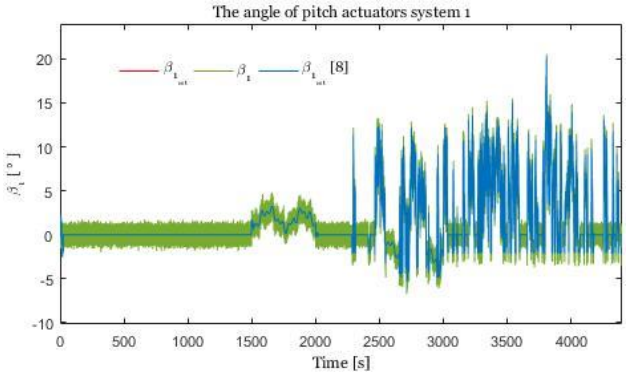

Figure 6. Pitch actuators system 1 angle β_1 and her estimated β_{1est} in terms of time.

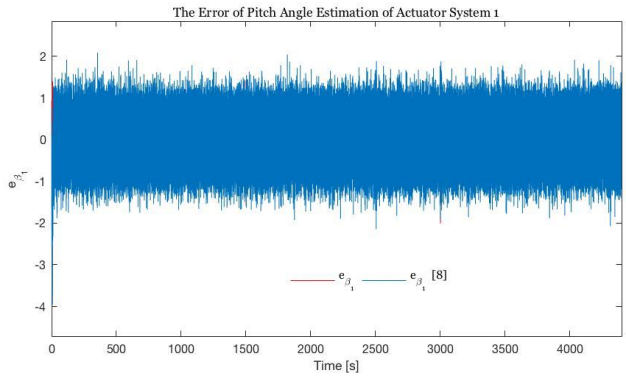

Figure 7. Error of estimation of pitch actuators system 1 $e_{\beta 1}$ in terms of time.

Moreover, following Figure 6, the following figures show the pitch actuators system 1 angle estimation β_{1est}, indicating the effectiveness of our proposed estimation strategy:

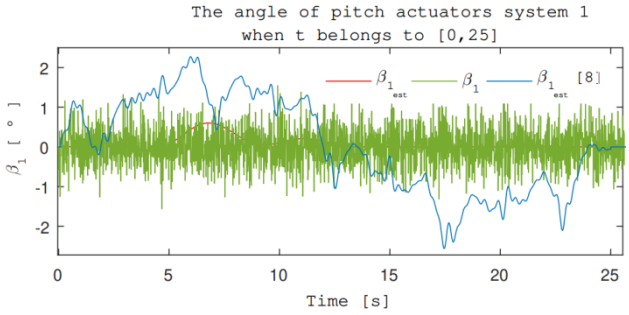

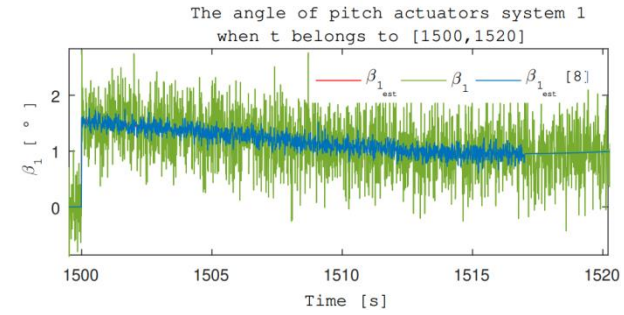

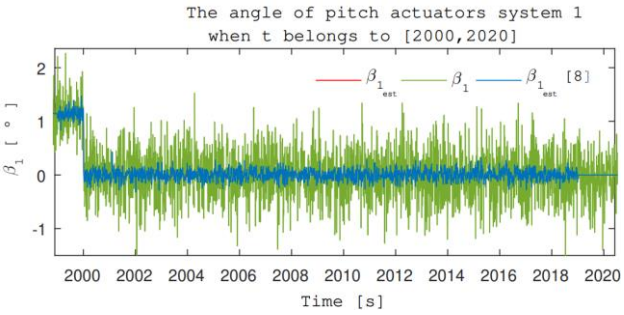

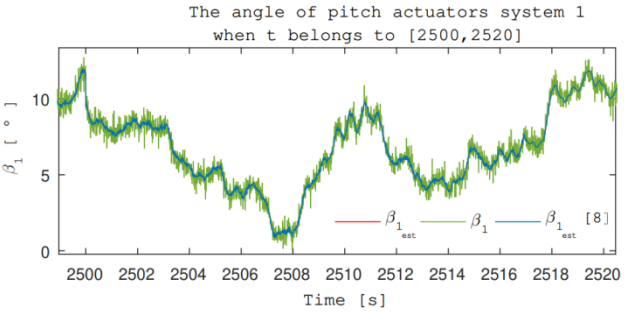

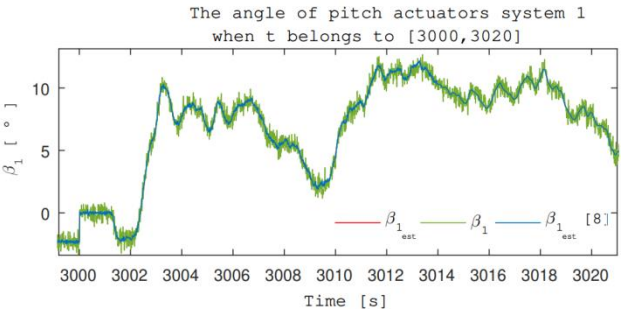

Pitch actuators system 2 angle β2

Figures 8 and 9 respectively show the pitch actuators system 2 angle estimation $\hat{\beta}_2$ and the error estimation $e_{\hat{\beta}_2}$ with the proposed PMI observer, where $\hat{\beta}_2 = \beta_{2_{est}}$ and $e_{\beta_{2_{est}}} = \beta_2 - \hat{\beta}_2$. The simulation shows that our proposed approach outperforms some existing approaches [8]:

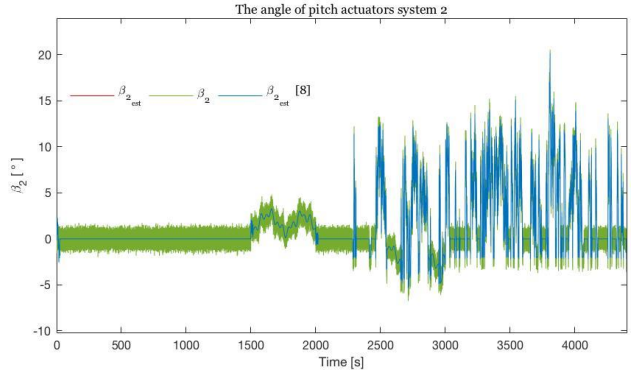

Figure 8. Pitch actuator system 2 angle β_2 and estimated β_{2est} in terms of time.

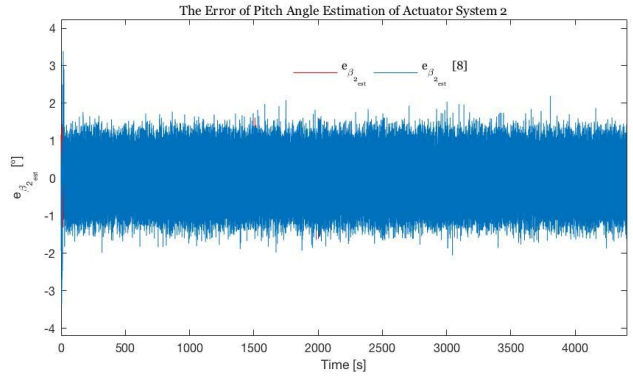

Figure 9. Estimation error of pitch angle actuators system 2 $e_{\beta 2est}$ in terms of time.

Moreover, following Figure 8, the following figures show the pitch actuator system 2 angle estimation β_{2est}, indicating the effectiveness of our proposed estimation strategy:

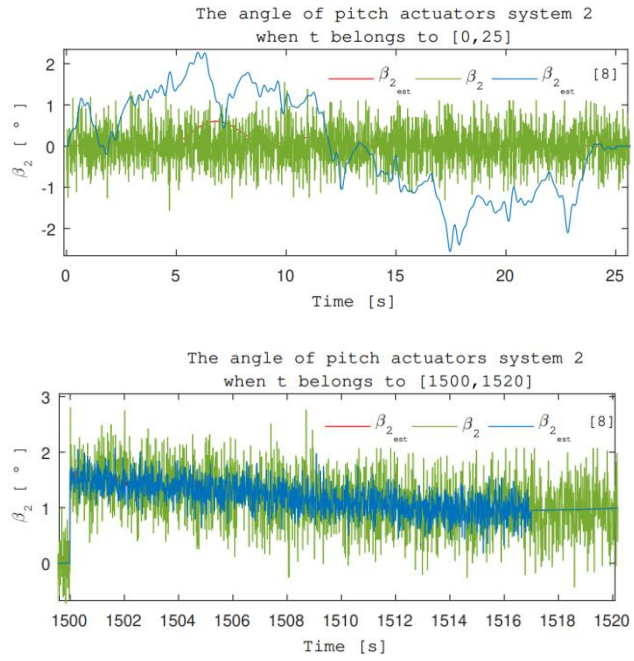

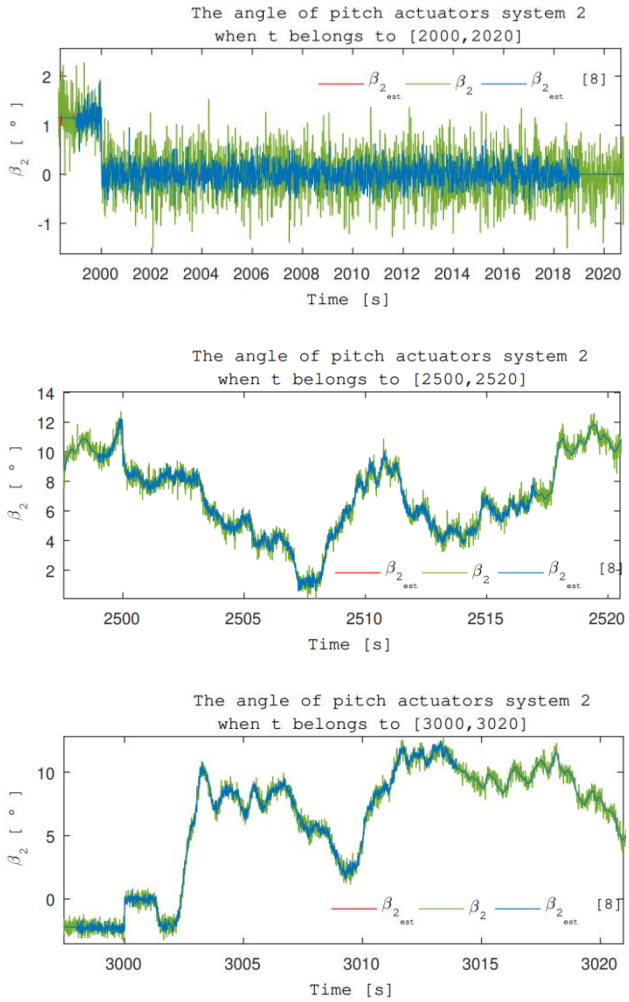

Pitch actuator system 3 angle β3

Figures 10 and 11 respectively show the pitch actuator system 2 angle estimation $\hat{\beta}_3$ and the error estimation $e_{\hat{\beta}_3}$ with the proposed PMI observer, where $\hat{\beta}_3 = \beta_{3_{est}}$ and $e_{\beta_{3est}} = \beta_3 - \hat{\beta}_3$. The simulation shows that our proposed approach outperforms some existing approaches [8]:

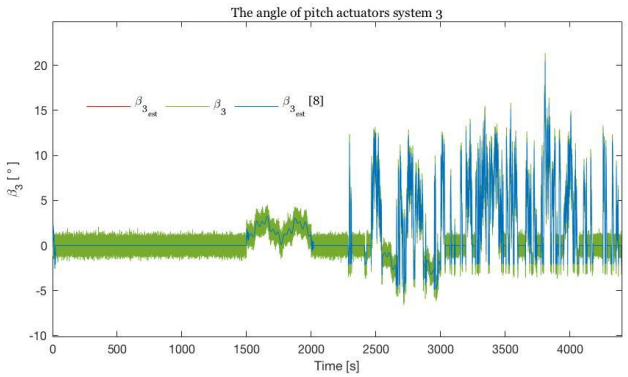

Figure 10. The pitch actuators system 3 angle β_3 and her estimated β_{3est} in terms of time.

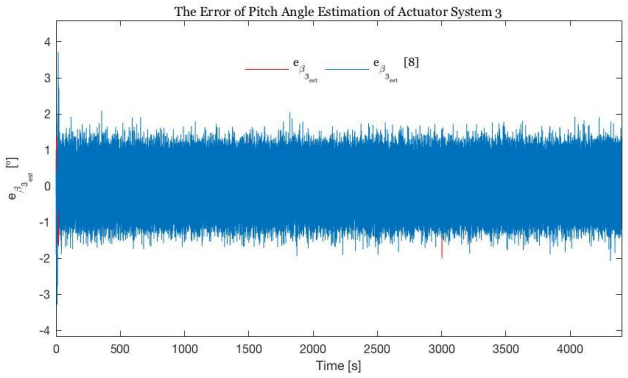

Figure 11. Error of estimation of pitch angle actuators system 3 $e_{\beta 3est}$ in terms of time.

Moreover, following Figure 10, the following figures show the pitch actuator system 3 angle estimation β_{3est}, indicating the effectiveness of our proposed estimation strategy:

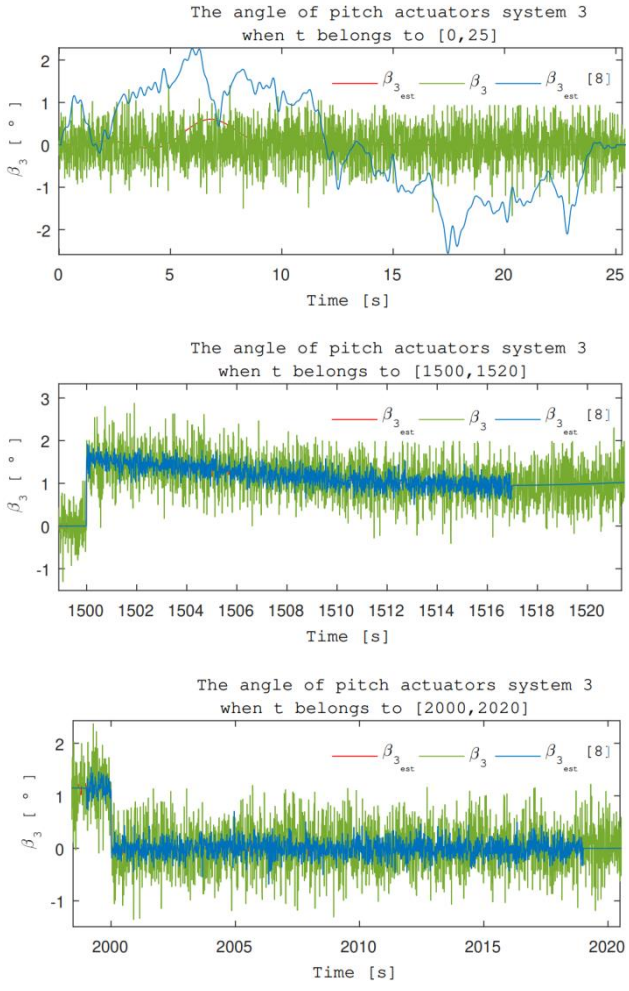

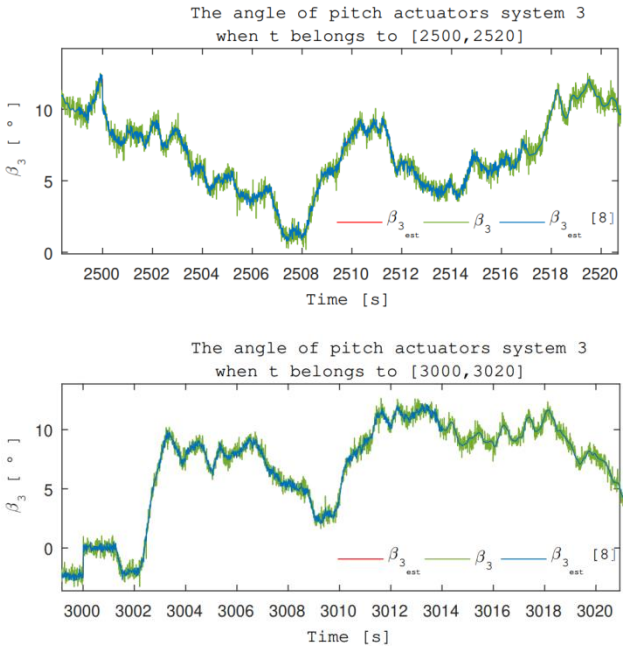

Generator torque τg

Figure 12 and 13 respectively show the generator torque estimation $\hat{\tau}_g$ and the error estimation $e_{\hat{\tau}_g}$ with the proposed PMI observer, where $\hat{\tau}_g = \tau_{g_{est}}$ and $e_{\tau_{gest}} = \tau_g - \hat{\tau}_g$. The simulation shows that our proposed approach outperforms some existing approaches [8]:

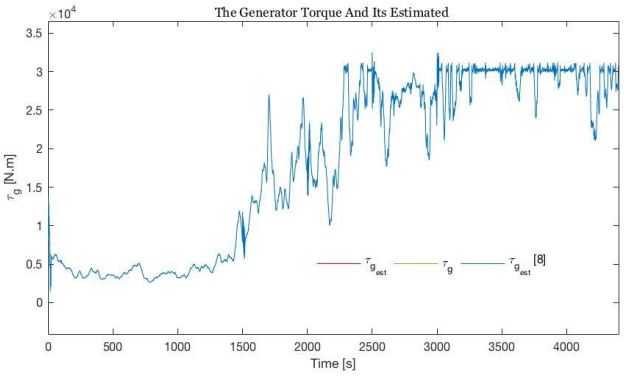

Figure 12. Generator torque τ_g and her estimated $\tau_{g,est}$ in terms of time.

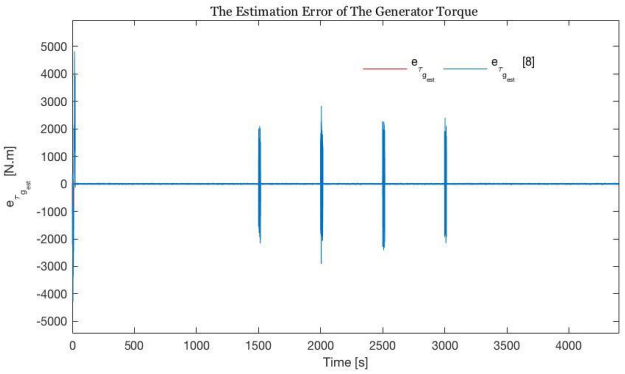

Figure 13. Error of estimation of generator torque $e_{\tau g,est}$ in terms of time.

Moreover, following Figure 13, the following figures show the generator torque estimation $\tau_{g,est}$, indicating the effectiveness of our proposed estimation strategy:

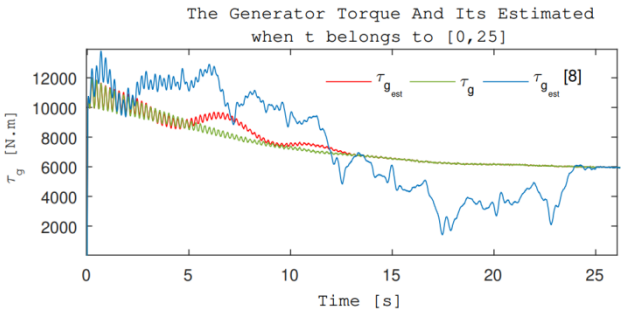

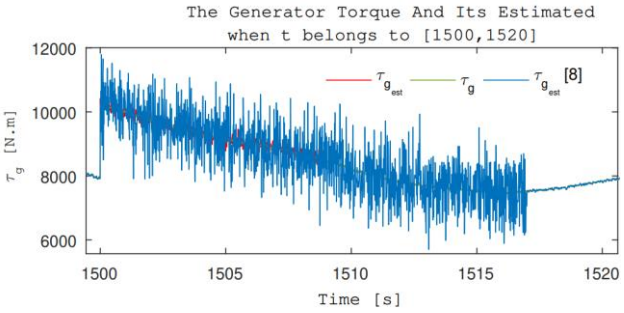

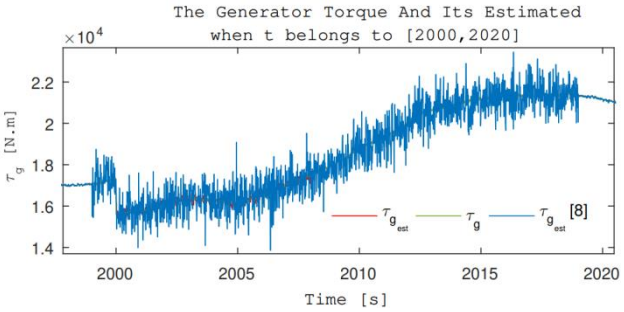

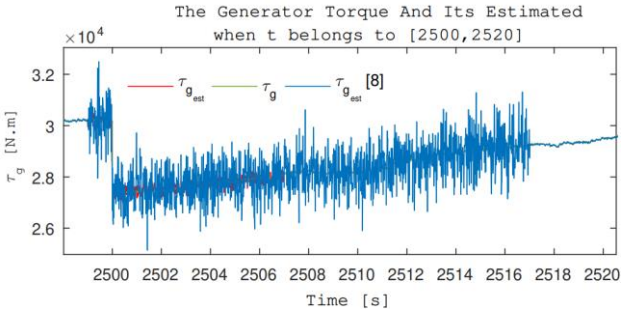

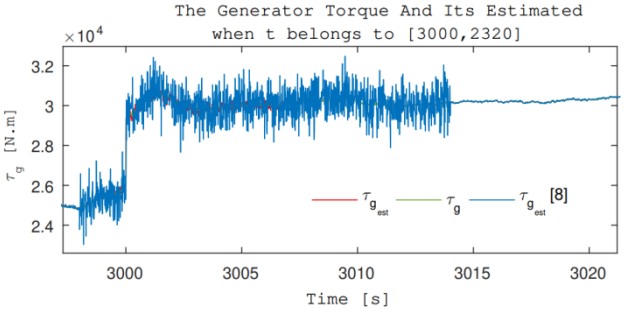

Generator speed ωg

Figure 14 and 15 respectively show the generator speed estimation $\hat{\omega}_g$ and the error estimation $e_{\hat{\omega}_g}$ with the proposed PMI observer, where $\hat{\omega}_g = \omega_{g_{est}}$ and $e_{\omega_{gest}} = \omega_g - \hat{\omega}_g$. The simulation shows that our proposal outperform estimate robust than some existing approach in the literature [8]:

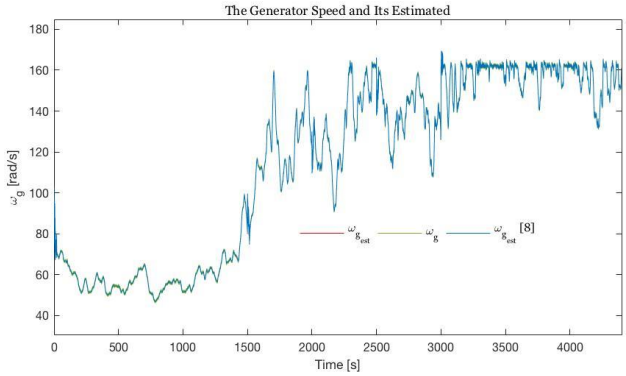

Figure 14. Generator speed ω_g and her estimated $\omega_{g,est}$ in terms of time.

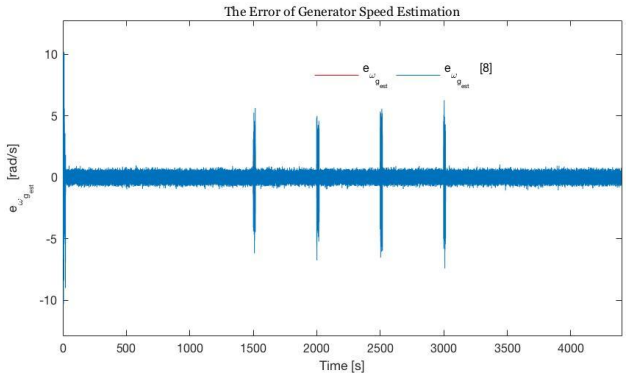

Figure 15. Error of estimation of generator speed $e_{\omega g,est}$ in terms of time.

Following figure 14, the following figures show the generator speed estimation $\omega_{g,est}$, indicating the effectiveness of our proposed estimation strategy:

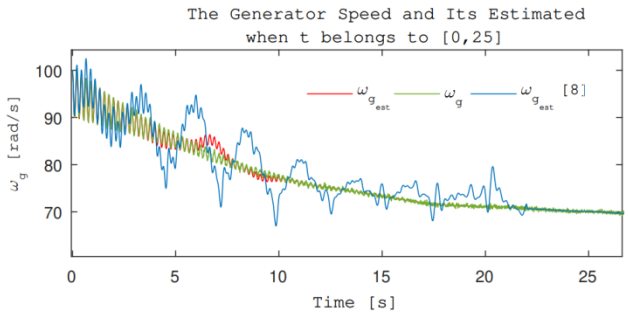

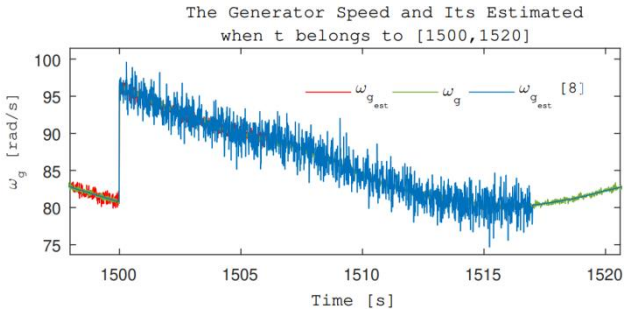

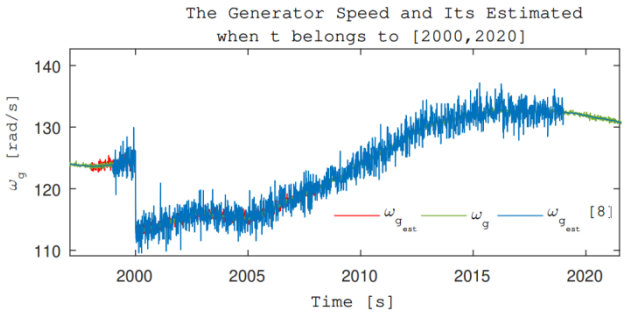

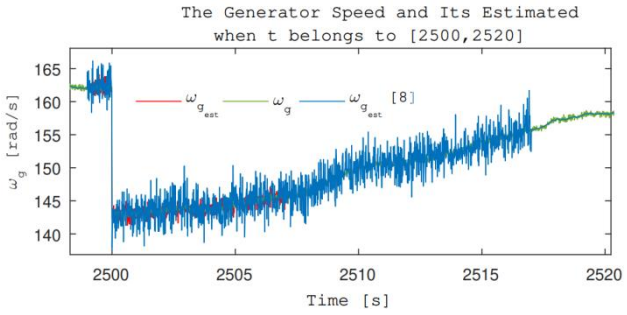

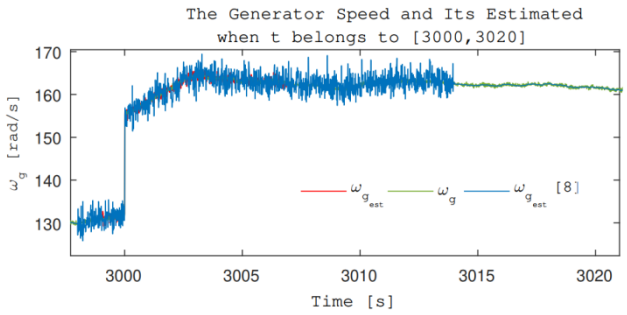

Rotor speed ωr

Figure 16 and 17 respectively show the rotor speed estimation $\hat{\omega}_r$ and the error estimation $e_{\hat{\omega}_r}$ with the proposed PMI observer, where $\hat{\omega}_r = \omega_{r_{est}}$ and $e_{\omega_{rest}} = \omega_r - \hat{\omega}_r$. The simulation shows that our proposed approach outperforms some existing approaches [8]:

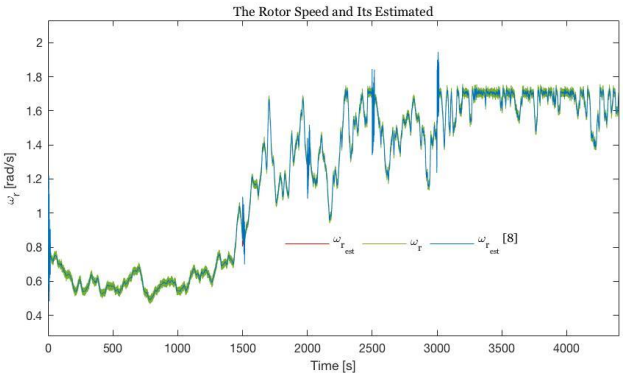

Figure 16. Rotor speed ω_r and her estimated $\omega_{r,est}$ in terms of time.

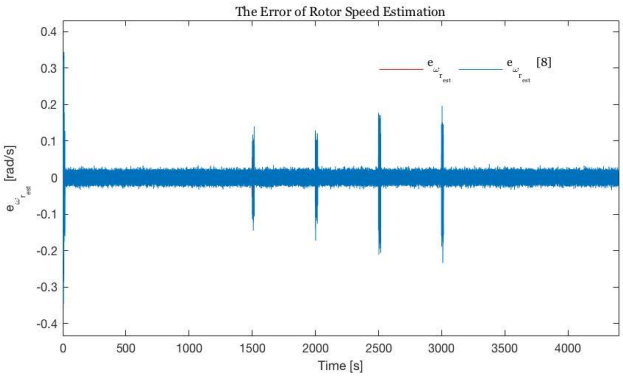

Figure 17. Error of estimation of rotor speed $e_{\omega r,est}$ in terms of time.

Following figure 16, the following figures show the rotor speed estimation $\omega_{r,est}$, indicating the effectiveness of our proposed estimation strategy:

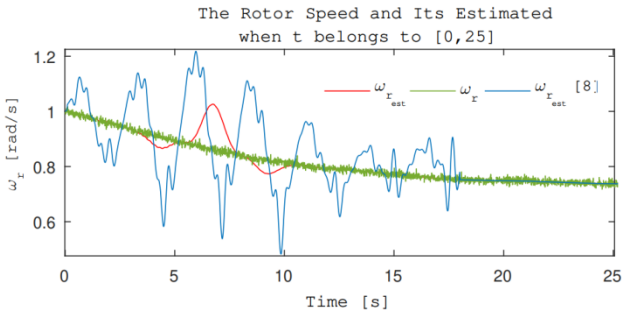

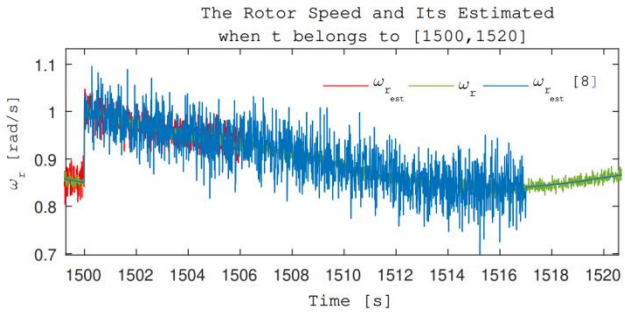

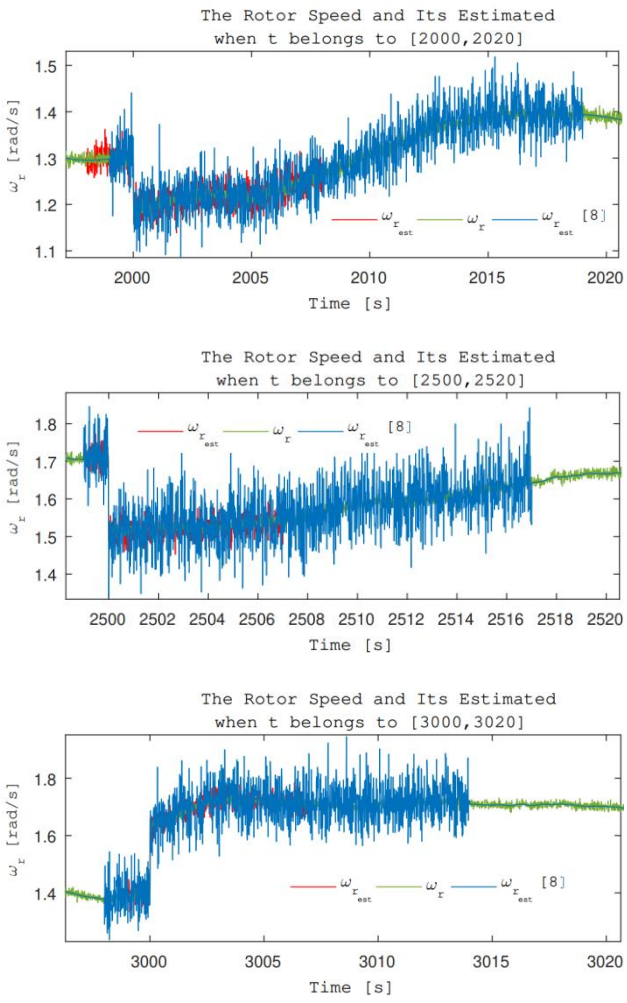

Sensor fault fs

Figure 18 shows the sensor fault estimation $\hat{f}_s$ with the proposed PMI observer, where $\hat{f}_s = f_{s_{est}}$. The simulation shows that our proposed approach outperforms some existing approaches [8]:

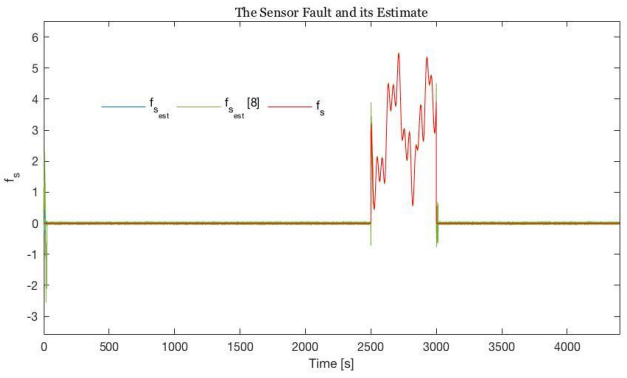

Figure 18. Sensor fault f_s and her estimated $f_{s,est}$ in terms of time.

Following Figure 18, the following figures show the sensors fault estimation $f_{s,est}$, indicating the effectiveness of our proposed estimation strategy:

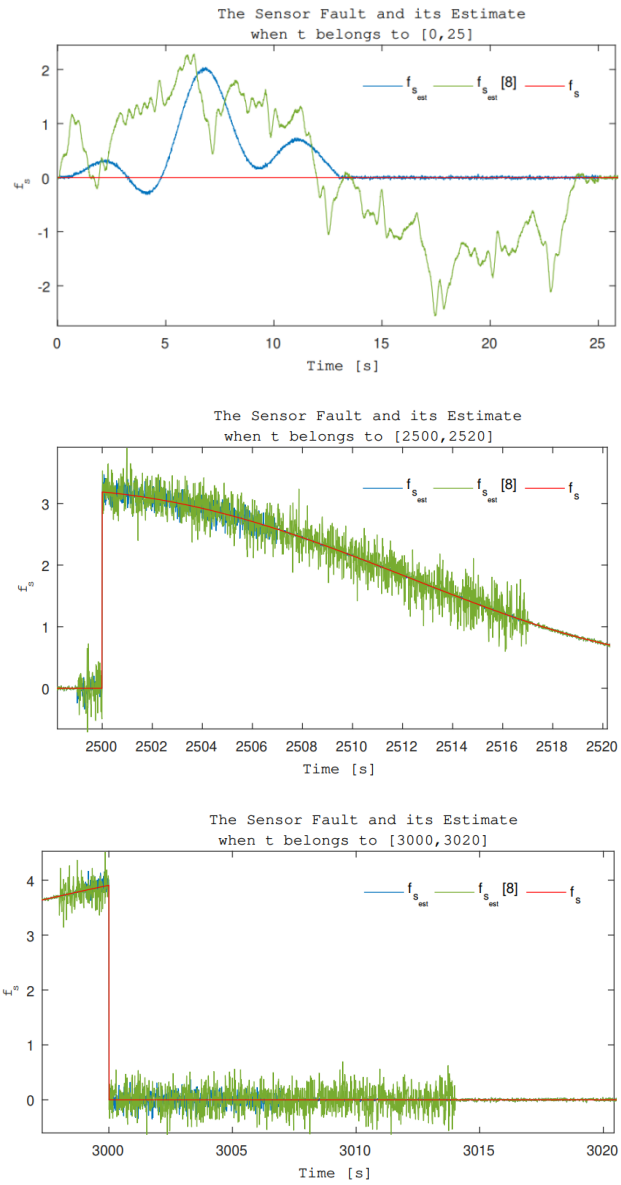

Actuators fault fa

Figure 19 shows the actuator fault estimation $\hat{f}_a$ with the proposed PMI observer, where $\hat{f}_a = f_{a_{est}}$. The simulation shows that our proposed approach outperforms some existing approaches [8]:

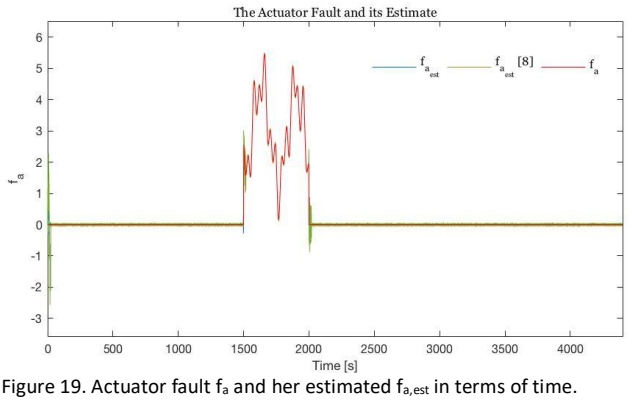

Figure 19. Actuator fault f_a and her estimated $f_{a,est}$ in terms of time.

Following figure 19, the following figures show the actuator fault estimation $f_{a,est}$, indicating the effectiveness of our proposed estimation strategy:

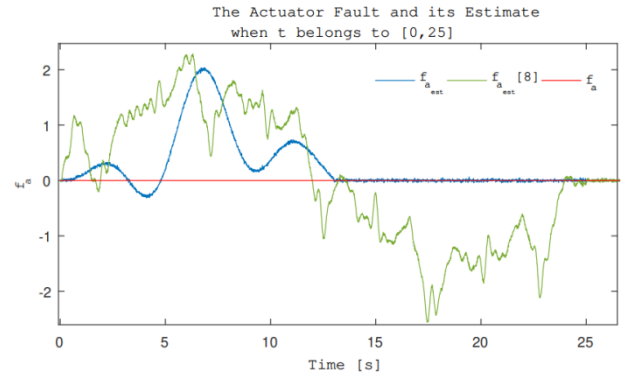

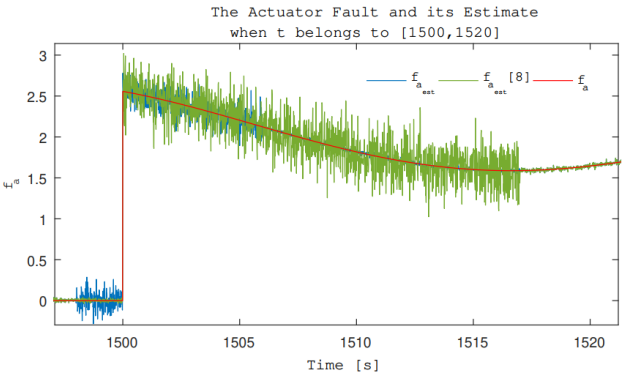

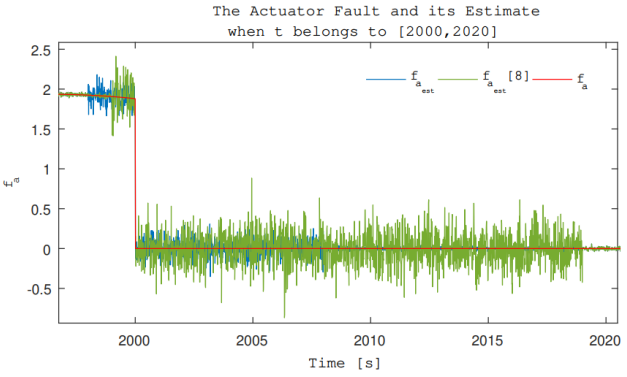

Finally, this proposed FDI approach can effectively estimate all states of the wind turbine system (13) while isolating actuator and sensorfaults. However, the sliding mode observer proposed in [8] is very sensitive to changes due to random noise and unusual defects, and the simulations are conducted to test the efficiency SMO using typical (i.e., triangular and rectangular) defects without noise. Consequently, the proposed PMI observer is more efficient and robust than the SM observer in estimating and detecting wind turbine system faults.

Conclusion

Fault detection and isolation in wind turbines is addressed through the use of the Proportional Multi-Integral Observer. First, the wind turbine system model was linearized using the Takagi-Sugeno (TS) approach based on the Lyapunov stability theory and LMI condition. We then consider a PMI observer for the T-S fuzzy model to estimate both actuator and sensor faults. The k^{th} derivatives of the actuators and sensor faults are not equal to zero and are bounded norms. However, based on the Lyapunov stability theory and L_2 performance analysis, design conditions are established in LMIs formulations. Finally, simulation results show our proposed approach outperforms some existing approaches.

References

[1] B. W. Ang, and Zhang, F. Q. “A survey of index decomposition analysis in energy and environmental studies,” *Energy*, vol. 25, no 12, pp. 1149-1176, 2000.
doi: 10.1016/S0360-5442(00)00039-6

[2] V. Fthenakis, and H. C. Kim, “Land use and electricity generation: A life-cycle analysis,” *Renewable and Sustainable Energy Reviews*, vol. 13, no 6-7, pp. 1465-1474 ,2009.
doi: 10.1016/j.rser.2008.09.017

[3] Sawin, L. Janet, Sverrisson, Freyr, Seyboth, Kristin, Adib, Rana, Murdock, E. Hannah, Lins, Christine, Edwards, Isobel, Hullin, Martin, Nguyen, H. Linh, Prillianto, S. Satrio, Satzinger, Katharina, Appavou, Fabiani, Brown, Adam, Chernyakhovskiy, Ilya, Logan, Jeffrey, Milligan, Michael, Zinaman, Owen, Epp, Baerbel, Huber, Lon, Lyons, Lorcan, Nowak, Thomas, Otte, Pia, Skeen, Jonathan, Sovacool, Benjamin, Witkamp, Bert, Musolino, Evan, Brown, Adam, Williamson, E. Laura, Ashworth, Lewis, Mastny, and Lisa, *Renewables 2017 Global Status Report*. Paris: REN21 Secretariat, 2017.

[4] J. K. Kaldellis, and D. Zafirakis, “The wind energy (r) evolution: A short review of a long history,” *Renewable Energy*, vol. 36, no 7, pp. 1887-1901, 2011.
doi: 10.1016/j.renene.2011.01.002

[5] W. Musial., and S. Butterfield “Future for offshore wind energy in the United States,” In proceeding of *Energy Ocean 2004*, Florida, June.28-29, 2004, pp. 4-6.
doi: 10.1002/9781118701638.ch1

[6] J. M. Jonkman, “Dynamics modeling and loads analysis of an offshore floating wind turbine,” 2007. Vol. 68. No. 11.

[7] P. Tavner, “Offshore Wind Turbines: Reliability, availability and maintenance ,” The Institution of Engineering and Technology, London, UK, 2012.

doi: 10.1049/PBRN013E_ch7

[8] M. Rahnavard, H. Yazdi, M Reza, and M Ayati, "On the development of a sliding mode observer-based fault diagnosis scheme for a wind turbine benchmark model," *Energy Equipment and Systems*, vol. 5, no 1, pp. 13-26, 2017.

[9] P. F. Odgaard, J. Stoustrup, and M Kinnaert, "Fault tolerant control of wind turbines-a benchmark model," In proceedings of *the IEEE International Conference on Control Applications (CCA)*, Hyderabad, India, Aug. 28-30, 2013, pp. 155-160. doi:10.1109/CCA.2013.6662784

[10] H. Toubakh, and M. Sayed-Mouchaweh, "Hybrid dynamic data-driven approach for drift-like fault detection in wind turbines," *Evolving Systems*, vol. 6, no 2, pp. 115-129, 2015. doi: 10.1007/s12530-014-9119-8

[11] S. Yin, G. Wang, and H. R. Karimi, "Data-driven design of robust fault detection system for wind turbines," *Mechatronics*, vol. 24, no 4, pp. 298-306, 2014. doi: 10.1016/j.mechatronics.2013.11.009

[12] F. Yassine, and B. Ismail, "Hybrid classifier for fault detection and isolation in wind turbine based on data-driven," in proceeding of *Intelligent Systems and Computer Vision (ISCV)*, Fez, Morocco, April 17-19, 2017. pp. 1-8. doi: 10.1109/ISACV.2017.8054976

[13] I. V. de Bessa, R. M. Palhares, M. F. S. V. D'Angelo, and Chaves J. E. Filho, "Data-driven fault detection and isolation scheme for a wind turbine benchmark," *Renewable Energy*, vol. 87, pp. 634-645, 2016. doi: 10.1016/j.renene.2015.10.061

[14] X. Zhang, Q. Zhang, S. Zhao, R. M. Ferrari, M. M. Polycarpou, and T. Parisini, "Fault detection and isolation of the wind turbine benchmark: An estimation-based approach," *IFAC Proceedings Volumes*, pp. 8295-8300, 2011. doi: 10.3182/20110828-6-IT-1002.02808

[15] W. Chen, S. X. Ding, A. Haghani, A. Naik, A. Q. Khan, and S. Yin, "Observer-based FDI schemes for wind turbine benchmark," *IFAC Proceedings Volumes*, vol. 44, no 1, pp. 7073-7078, 2011. doi: 10.3182/20110828-6-IT-1002.03469

[16] F. Kiasi, J. Prakash, S. Shah, and J. M. Lee, "Fault detection and isolation of benchmark wind turbine using the likelihood ratio test," *IFAC Proceedings Volumes,* pp. 7079-7085, 2011. doi: 10.3182/20110828-6-IT-1002.03535

[17] H. Sanchez, T. Escobet, V. Puig, and P. F. Odgaard, "Fault diagnosis of an advanced wind turbine benchmark using interval-based ARRs and observers," *IFAC Proceedings Volumes*, vol. 47, no. 3, pp.4334-4339, 2014. doi: 10.3182/20140824-6-ZA-1003.01668

[18] P. F. Odgaard , J. Stoustrup, R. Nielsen, and C. Damgaard, "Observer based detection of sensor faults in wind turbines," In proceedings of European wind energy conference. 2009. pp. 4421-4430.

[19] D. Rotondo, V. Puig, J. M. A. Valle, and F. Nejjari, "FTC of LPV systems using a bank of virtual sensors: Application to wind turbines," In proceeding of *Control and Fault-Tolerant Systems (SysTol)*, Nice, France, Oct 9-11, 2013, pp. 492-497. doi: 10.1109/SysTol.2013.6693844

[20] S. Simani, S. Farsoni, and P. Castaldi, "Fault diagnosis of a wind turbine benchmark via identified fuzzy models," *IEEE Transactions on Industrial Electronics*, vol. 62, no. 6, pp. 3775-3782, 2015. Doi: 10.1109/TIE.2014.2364548

[21] G. R. Duan, and H. H.LMIs Yu, in control systems: analysis, design and applications. CRC press, 2013.

[22] L. P. K. Johnson, "Control of wind turbines. approaches, challenges, and recent developments," *IEEE Control systems magazine*, 2011, vol. 58, no 4, pp. 44-62.

[23] P. F. Odgaard, J. Stoustrup, and M Kinnaert,. "Fault-tolerant control of wind turbines: A benchmark model," *IEEE Transactions on Control Systems Technology*, vol. 21, no 4, pp. 1168-1182, 2013. doi: 10.3182/20090630-4-ES-2003.00026

[24] K. Tanaka, and H. O. Wang, "Fuzzy control systems design and analysis: a linear matrix inequality approach," *John Wiley and Sons*, 2004. doi: 10.1016/S0005-1098(03)00188-2

[25] T. Takagi, and M. Sugeno, "Fuzzy identification of systems and its applications to modeling and control," *Readings in Fuzzy Sets for Intelligent Systems, Pages 387-403*, no 1, pp.387-403, 1993. doi: 10.1016/B978-1-4832-1450-4.50045-6

[26] M. Sugeno, and G. T. Kang, "Fuzzy modelling and control of multilayer incinerator,"*Fuzzy sets and systems*, vol. 18, no 3, pp. 329-345, 1986. doi: 10.1016/0165-0114(86)90010-2

[27] H. O. Wang, K. Tanaka, , and M. Griffin, "Parallel distributed compensation of nonlinear systems by Takagi-Sugeno fuzzy model," In proceedings of IEEE International Conference on Fuzzy Systems, Yokohama, Japan, March.20-24, 1995. pp. 531-538. doi: 10.1109/FUZZY.1995.409737

[28] Z. Gao, S. X. Ding, and Y. Ma, "Robust fault estimation approach and its application in vehicle lateral dynamic systems," *Optimal Control Applications and Methods*, vol. 28, no 3, pp. 143-156, 2007.

doi: 10.1002/oca.786

[29] T. Youssef, M. Chadli, H. R. Karimi, and M. Zelmat, "Design of unknown inputs proportional integral observers for TS fuzzy models," *Neurocomputing*, vol. 123, pp. 156-165, 2014. doi: 10.1016/j.neucom.2013.06.024